Improving near-field confinement of a bowtie aperture using surface plasmon polaritons

Pornsak Srisungsitthisunti,[1] Okan K. Ersoy,[2] and Xianfan Xu[1,a)]
[1]*School of Mechanical Engineering and Birck Nanotechnology Center, Purdue University, West Lafayette, Indiana 47907, USA*
[2]*School of Electrical and Computer Engineering, Purdue University, West Lafayette, Indiana 47907, USA*

(Received 25 March 2011; accepted 6 May 2011; published online 1 June 2011)

Bowtie aperture is known to produce subdiffraction-limited optical spot with high intensity. In this work, we investigate integrating a bowtie aperture with circular grooves to reduce the divergence of the near-field produced by the bowtie aperture. Numerical results indicate that surface waves reflected from circular grooves improve the field confinement of a bowtie aperture along the polarization axis. These circular grooves with period near half the wavelength of surface plasmon polaritons reduce the spot size by as much as 40% at distances between 20 and 100 nm from the surface and create a more symmetrical optical spot. © *2011 American Institute of Physics*. [doi:10.1063/1.3595412]

Bowtie apertures have been shown to achieve extraordinary transmission and produce subdiffraction-limited optical spot for near-field applications such as data storage, near-field scanning optical microscopy (NSOM), and nanolithography.[1–3] A bowtie aperture, illustrated in Fig. 1(a), can be designed to produce a subdiffraction-limited optical spot shown in Fig. 1(b), which is determined by the gap between the two tips of the bowtie aperture. The field intensity at the bowtie gap is orders of magnitude higher than the incident field. Moreover, an array of bowtie apertures can generate multiple light spots for sensing[4] and for parallel processes.[5] However, the field beyond the surface of a bowtie aperture is subjected to strong divergence. Consequently, the working distance of the bowtie is limited to the very near-field. The bowtie apertures are often used in contact with another surface to obtain a subdiffraction spot.[5–7]

In this work, we investigate a method to reduce near-field divergence of a bowtie aperture by surrounding the bowtie aperture with concentric grooves on the exit side of the metal film as illustrated in Fig. 1(c). Surface plasmon polaritons (SPPs) are excited by the incident light at the bowtie aperture. The grooves partially reflect and scatter SPPs toward the bowtie, modifying the field divergence. When designed properly, these grooves effectively reduce the spot size of the propagating field. It should be noted that the transmission of a bowtie aperture can be enhanced by placing corrugations on the incident side,[8] which act as gratings that collect more light. These gratings are effective in improving the transmission but are not intended for narrowing field concentration.

Grooves on the exit side of a metal film have been suggested to obtain far-field collimation and focusing of a subwavelength hole or slit.[9–14] Most of these designs are based on SPP scattering and interference in the far-field. Each groove scatters the SPP waves into the propagating wave with a phase delay specified by the traveling distance from the hole or the slit. By adjusting relative positions of the grooves, a focused spot can be obtained by phase matching of the scattered SPPs.[9–14] However, this far-field focusing fundamentally limits the spot size to the diffraction limit. SPPs can also be excited inside narrow slits. A plasmonic lens can be designed to interfere SPPs emerging from concentric slits to produce a spot in the near-field.[15] Here we investigate how the SPPs can further reduce the near-field divergence from a bowtie aperture within a 100 nm distance from the exit surface. A small near-field spot beyond the exit plane is desirable for many applications requiring noncontact between the near-field optical element and the surface the light interacts with. For example, it will provide more positioning tolerance and design space in nanolithography,[5–7,15] data storage,[1,16] and NSOM.[2]

We first investigate the behavior of a two-dimensional (2D) slit-grooves structure, which provides an understanding

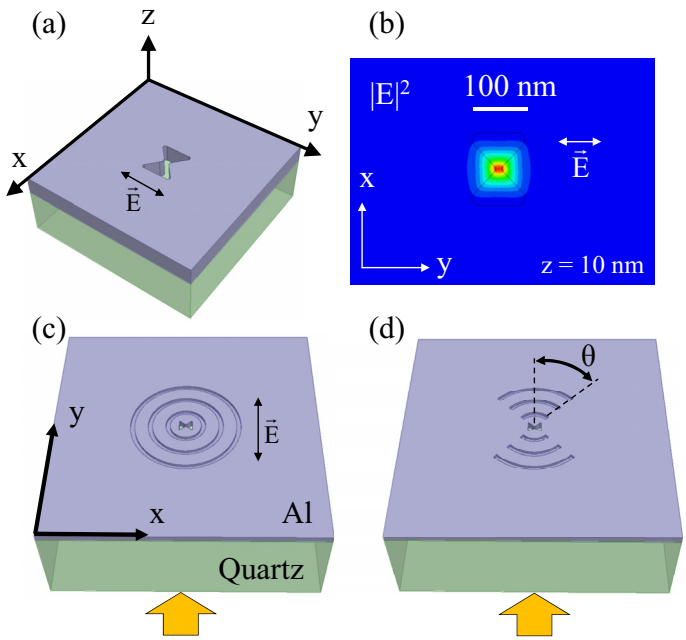

FIG. 1. (Color online) (a) Schematic of a bowtie aperture and (b) its corresponding $|E|^2$ calculated at 10 nm distance from the surface. Modified bowtie aperture with (c) full circular grooves and (d) partial circular grooves on the exit side of the film.

a)Author to whom correspondence should be addressed. Electronic mail: xxu@purdue.edu.

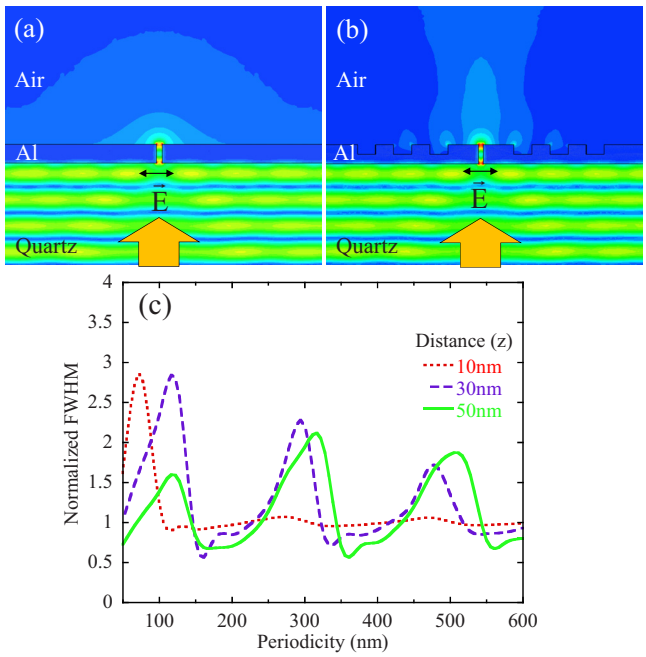

FIG. 2. (Color online) Normalized electric field distribution from (a) a single slit and (b) slit with exit grooves with 200 nm periodicity. The arrow indicates the light irradiation direction. (c) FWHM of the emerging field of structure in (b) normalized by (a) as a function of groove periodicity. The slits are illuminated by a 400-nm-wavelength linearly polarized light.

of the interaction between SPPs and a diverging near-field, and facilitates the design of the computationally more intensive three-dimensional bowtie-grooves structure. All the simulations were carried out using a finite element solver, HFSS™.[17] The grid size is adaptive with a smallest grid size of 2 nm in critical areas. Material properties are obtained from Ref. 18. A 30-nm-width slit in a 100-nm-thick aluminum film on a quartz substrate is illuminated by a TM-polarized 400-nm-wavelength plane wave. Since the surface grooves are designed to concentrate light in the near-field, the positions of the grooves are distributed evenly. For parametric studies, the periodicity of the grooves is varied from 50 to 600 nm with an increment of 25 nm. The depth of the grooves is fixed as half of the film thickness (50 nm) and the grooves' width is half the periodicity. For simplicity, the slit-to-groove distance is set equal to the periodicity.

Figures 2(a) and 2(b) compare the electric field distribution of the slit (only) and the slit with grooves. Clearly, the grooves create a directional field beaming in the propagating direction compared to a single slit. Figure 2(c) plots the full-width at half-maximum (FWHM) of the slit with grooves normalized to that of the single slit as a function of groove periodicity. The periodicities near 200 and 400 nm show significant FWHM reduction as much as 40%. The reduced FWHM repeats every 200 nm of periodicity, close to half the SPP wavelength (λ_{SPP}), which is 391 nm for Al/air interface. At these periodicities, the grooves produce standing waves matching the SPP wavelength. Superposition of these standing waves and the emerging field at the slit leads to a narrower field. When changing the film and media materials, we found that the optimum periodicities depend on the SPP wavelength which is a function of free space wavelength, metal film, and media properties.

Our optimized periodicity of about $\lambda_{SPP}/2$ differs from the results of far-field collimation by grooves for which the optimized grooves spacing is close to λ_{SPP}.[9–13] This is because the mechanism of reducing the near-field confinement is different from diffraction in far-field collimation. For far-field collimation, the relative phase difference of waves produced by each groove is 2π to achieve constructive interference. This is equivalent to a groove spacing of λ_{SPP}. On the other hand, for focusing light in the near-field, since the SPPs are initially excited at the slit and travel to the grooves, the groove spacing of $\lambda_{SPP}/2$ provides 2π phase modulation when the wave propagates to and reflects from the groove.

A close examination of Fig. 2(b) indicates that SPP waves are excited at the edges of each groove and stronger fields are located at the closer edges to the central slit. Therefore, the distances between these edges and the central slit have the largest effect on the superimposed field. On the other hand, the width of the groove controls the relative phase of the SPPs generated at the two edges of each groove. The depth of the grooves also influences the relative phase of the SPPs. For a deeper groove, SPPs propagate and reflect inside the groove through a longer distance, leading to an increased phase delay.[14] In our case, the film thickness is much smaller than the wavelength, so the groove depth is less influential.

Next, we consider a bowtie aperture surrounded by concentric grooves as shown in Fig. 1(c). In our earlier studies,[19] the geometry of a bowtie aperture has been optimized to achieve resonant condition and maximum transmission at 400 nm wavelength. The following parameters are used for the bowtie aperture, the length is 100 nm on all sides with a 45° angle, and the gap is 30 nm which is a dimension readily fabricated using focused ion beam milling. The bowtie aperture is made in 100-nm-thick aluminum film deposited on a quartz substrate. The grooves have a periodicity of 200 nm, depth of 50 nm, width of 100 nm, and the bowtie to groove (center-to-center) distance of 200 nm. The bowtie aperture is excited with a 400-nm-wavelength plane-wave polarized along the y-direction.

The calculation results indicate a smaller optical spot along the y-direction when the grooves are present. Figure 3 compares the field distributions with and without grooves. A single bowtie produces an elliptical spot beyond the exit plane due to a strong dipolelike field with a larger size in the y-direction. This asymmetry becomes more severe at longer distances as shown in Figs. 3(a)–3(c). When the grooves are present, the SPPs are partially reflected back toward the bowtie. With periodicity close to half the SPP wavelength, the reflected SPPs superimpose with the propagating field. The resulting FWHM is smaller along the *y*-axis, and the spot becomes considerably more symmetric. The FWHMs in the y-direction are reduced by 15%–35% at distances 20–100 nm from the surface.

Since the grooves only produce strong effect along the *y*-axis, we also investigated partial grooves as shown in Fig. 1(d). Figure 4 compares the bowtie-grooves structure with different groove coverage angles as defined in Fig. 1(d). It shows that partial grooves with a 45° angle are as effective as full grooves for reducing the spot size. The grooves with an angle smaller than 45° reflect less SPPs, resulting in less confinement in the field. Figure 4 also shows that at distances 60–80 nm, the grooves are most effective and reduce the FWHM by 35%. At a distance smaller than 20 nm, the field produced by the bowtie is extremely strong so that the FWHM is less affected by the SPPs, similar to the case of 2D

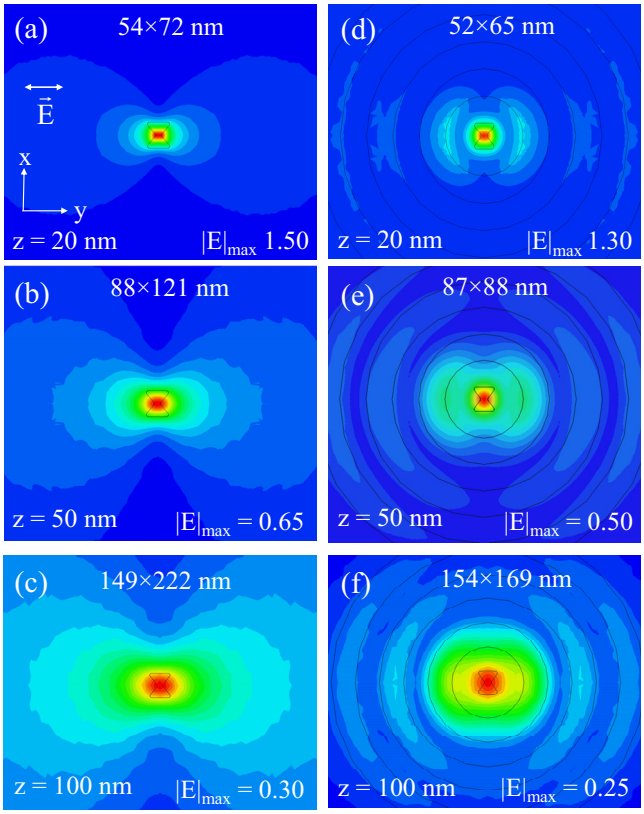

FIG. 3. (Color online) Comparison of electric field distributions of [(a)–(c)] single bowtie aperture and [(d)–(f)] bowtie aperture with circular grooves at working distances of 20, 50, and 100 nm. The bowtie apertures are excited by a plane-wave whose electric field is linearly polarized along the *y*-axis.

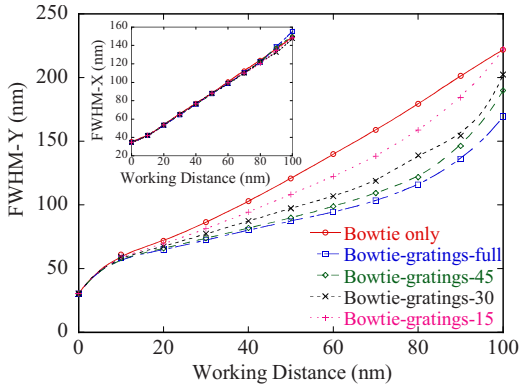

FIG. 4. (Color online) FWHM of $|E|^2$ along y-direction and x-direction (inset) of a bowtie and a bowtie surrounded by grooves with different angular coverage.

slit-grooves. The inset of Fig. 4 shows that the dimension in the x-direction is essentially not affected due to the lack of SPPs.

In summary, we proposed a method for reducing the near-field divergence of the subdiffraction-limited spot created by a bowtie aperture, using SPPs reflected from grooves surrounding the bowtie aperture. The near-field confinement is based on superposition of the central field and the reflected SPPs. The results confirm a spot reduction as much as 40% for the 2D slit-grooves and 35% for the bowtie-grooves structure. This approach is especially suitable for the bowtie aperture where the divergence is strong along the polarization axis, producing a more symmetric optical spot. These simple additions make bowtie aperture a more attractive device for near-field applications where direct contact between the bowtie aperture and another surface is not desirable.

The authors gratefully acknowledge the support of the National Science Foundation (Grant No. DMI-0707817), the Defense Advanced Research Projects Agency (Grant No. N66001-08-1-2037), and the AFOSR-Multidisciplinary University Research Initiative program (Grant No. FA9550-08-1-0379).

[1]K. Şendur, W. Challener, and C. Peng, J. Appl. Phys. **96**, 2743 (2004).
[2]L. Wang and X. Xu, Appl. Phys. Lett. **90**, 261105 (2007).
[3]L. Wang, S. M. Uppuluri, E. X. Jin, and X. Xu, Nano Lett. **6**, 361 (2006).
[4]E. Kinzel and X. Xu, Opt. Lett. **35**, 992 (2010).
[5]S. M. V. Uppuluri, E. C. Kinzel, Y. Li, and X. Xu, Opt. Express **18**, 7369 (2010).
[6]N. Murphy-DuBay, L. Wang, and X. Xu, Appl. Phys. A: Mater. Sci. Process. **93**, 881 (2008).
[7]Y. Kim, S. Kim, H. Jung, E. Lee, and J. W. Hahn, Opt. Express **17**, 19476 (2009).
[8]E. C. Kinzel, P. Srisungsitthisunti, Y. Li, A. Raman, and X. Xu, Appl. Phys. Lett. **96**, 211116 (2010).
[9]S. Kim, Y. Lim, H. Kim, J. Park, and B. Lee, Appl. Phys. Lett. **92**, 013103 (2008).
[10]H. J. Lezec, A. Degiron, E. Devaux, R. A. Linke, L. Martin-Moreno, F. J. Garcia-Vidal, and T. W. Ebbesen, Science **297**, 820 (2002).
[11]F. J. García-Vidal, L. Martín-Moreno, H. J. Lezec, and T. W. Ebbesen, Appl. Phys. Lett. **83**, 4500 (2003).
[12]L. Martín-Moreno, F. J. García-Vidal, H. J. Lezec, A. Degiron, and T. W. Ebbesen, Phys. Rev. Lett. **90**, 167401 (2003).
[13]F. Hao, R. Wang, and J. Wang, Opt. Express **18**, 15741 (2010).
[14]H. Shi, C. Du, and X. Luo, Appl. Phys. Lett. **91**, 093111 (2007).
[15]W. Srituravanich, L. Pan, Y. Wang, C. Sun, D. B. Bogy, and X. Zhang, Nat. Nanotechnol. **3**, 733 (2008).
[16]W. A. Challener, C. Peng, A. V. Itagi, D. Karns, W. Peng, Y. Peng, X. Yang, X. Zhu, N. J. Gokemeijer, Y. T. Hsia, G. Ju, R. E. Rottmayer, M. A. Seigler, and E. C. Gage, Nat. Photonics **3**, 220 (2009).
[17]Ansoft Inc., HFSS 12.1.1 software, 2009.
[18]P. B. Johnson and R. W. Christy, Phys. Rev. B **6**, 4370 (1972).
[19]L. Wang and X. Xu, Appl. Phys. A: Mater. Sci. Process. **89**, 293 (2007).